HANFORD IFRC QUARTERLY REPORT ~ October 2009

John M. Zachara and the IFRC Research Team
Pacific Northwest National Laboratory

I. Overview and Highlights

This Quarterly Report for the Hanford IFRC project summarizes significant progress for the period of July 2009 to October 2009. As stated in the previous quarterly report, the emphasis of this report is on modeling progress, but two major field experiments were also completed. Three major highlights deserve mention for this reporting period that will be discussed in sections that follow.

1. A large scale, non-reactive tracer experiment focused on dynamic geophysics data collection and monitoring was successfully performed in August 2009. The experiment involved the injection of Br^- spiked groundwater with significant salinity contrast followed by plume monitoring with multiple geophysics arrays, downhole ion selective electrodes, and laboratory analyses of Br. The experiment design was assisted by premodeling using updated hydrogeological parameters for the site determined by the first two tracer experiments.
2. Significant progress has been made on developing 3D distributions of hydraulic conductivity and other hydraulic parameters, incorporating these measures and their realizations into an updated and increasingly robust hydrologic model of the IFRC site, and using this model for plume/tracer experiment modeling and parameter optimization.
3. A preliminary IFRC geochemical model has been developed for coupled surface complexation (adsorption) and mass transfer based on robust laboratory experiments of disturbed grab samples and intact sediment cores. The sensitivity of model parameters has been numerically evaluated through application to various in-situ hydrogeochemical scenarios. It is now being applied for premodeling of U(VI) reactive transport experiments.

II. Significant Changes

There have been no significant changes to the project scope or objectives since the last quarterly report in July 2009.

III. Management & Operations

Management and operations of the Hanford IFRC have proceeded without major problems over the two past reporting quarters. Site completion, characterization, lab/field

experimentation, model and project spending has proceeded as planned, and the project overall is on schedule with milestones.

IV. Quarterly Highlights

Task 1. Project Management

IFRC project management is proceeding smoothly and there are no outstanding issues with finances, staffing, subcontracts, project productivity, site infrastructure or access, schedule, or modeling. The project team is actively working to complete manuscripts on the initial injection and passive experiments and development of improved site hydrogeologic and geochemical conceptual and numerical models. Active planning is underway for a field injection experiment involving lower concentrations of uranium to be conducted later in October.

Task 2. Site Design and Installation

No significant site design activities occurred during the fourth quarter, but design of the infiltration component of the field site will be initiated early in FY 2010. An array of temporary surface electrodes was installed for characterization of the well field and for measurements during the August geophysics injection experiment. The surface electrodes were removed in September, but their locations were identified with stakes and tags.

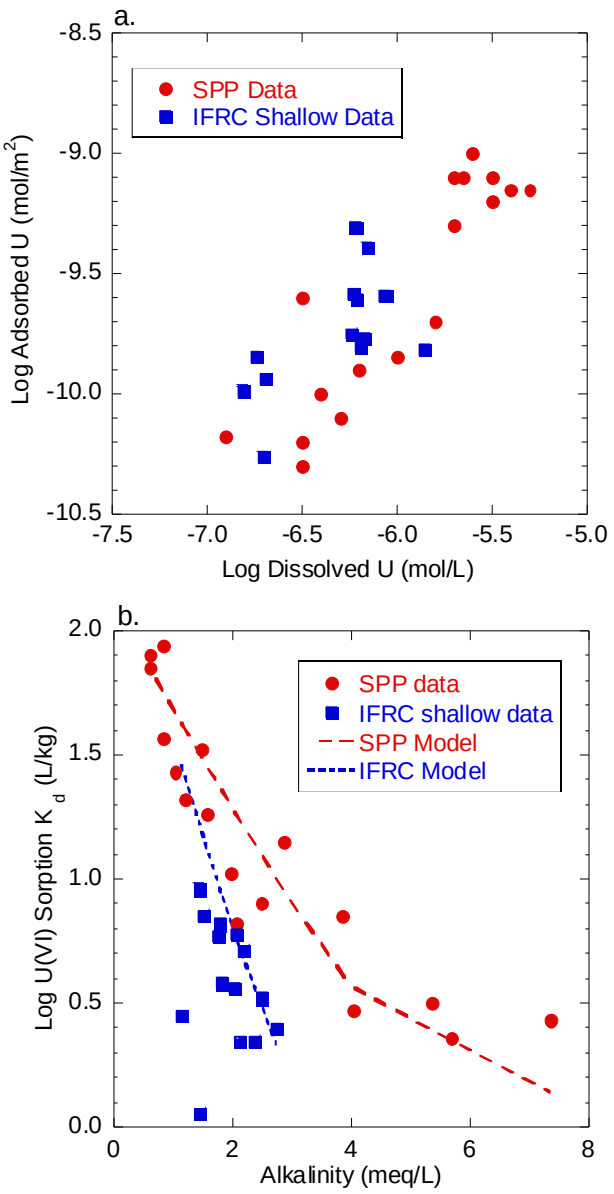

Figure 1. Experimentally determined and model-calculated U(VI) adsorption on smear-zone samples from six locations in the IFRC experimental domain (IFRC shallow data and Model, respectively). For comparison, experimentally determined and model-calculated U(VI) adsorption on vadose-zone sediments from the SPP (historic excavation immediately west of IFRC well #3-26) are also shown (Bond et al., 2008). Influence of U(VI) dissolved concentration (a) and alkalinity (b) on U(VI) adsorption. Model lines are spline fits through model-computed adsorption points.

Task 3. Website and Data Management

The IFRC database site was updated to increase functionality. It includes access for project participants to temperature and well data, geophysics results, borehole logs and other data. The database currently holds over fifty million records. The team is focused on integrating experimental data in a coherent framework.

Task 4. Field Site Characterization

Samples obtained from the IFRC well field during the drilling campaign continue to be characterized according to the Hydrologic and Geochemical Characterization Plan that is posted on the web. Phase I of the Characterization Plan has been completed and results are being incorporated into a series of manuscripts.

Geophysical Characterization

The first phase of this activity was completed as described in the last quarterly report. That activity involved the 3-D geophysical characterization of IFRC domain using the 840 down-hole ERT electrodes installed during well placement. Many thousands of measurements resulted from cross-electrode data collection that was inverted to yield a 3-D distribution map for electrical resistivity throughout the experimental site. These results are being incorporated into an interpretive manuscript for journal submission.

Laboratory measurements are underway this fiscal year to develop correlations between electrical resistivity and select hydrophysical properties of the sediments including grain size distribution. Such correlations will allow prediction of hydrophysical properties throughout the IFRC domain from non-invasive ERT measurements.

Geochemical Characterization (USGS summary)

Experiments conducted with the < 2 millimeter fraction of U(VI)-contaminated sediments collected from the smear zone at six locations within the IFRC domain showed that U adsorption generally increases with increasing concentration and decreasing alkalinity (Figure 1). Desorption of adsorbed contaminant U required at least 1000 hours to reach equilibrium. Much of the scatter apparent in the adsorbed *versus* dissolved U plot (panel A) is caused by variable alkalinity, which is the primary chemical control on U adsorption on these samples (Bond et al., 2008). The specific surface areas of the smear-zone composites are similar (10±1 m^2/g) and, therefore, scatter evident in the adsorbed U (expressed as K_d) *versus* alkalinity plot (Figure 1, Panel b) is likely caused by spatial variability in adsorption properties of sediments. Vadose-zone sediments from the South Process Pond (SPP) studied by Bond et al. (2008) had approximately twice the specific

surface area of the IFRC smear-zone composites. Values of K_d were not adjusted for differences in surface area and, therefore, differences between K_d values determined on SPP vadose-zone sediments and IFRC sediments cannot be used to assess differences in adsorption properties.

Uranium adsorption data for all IFRC smear-zone composite samples were combined and fitted to various surface complexation models. The modeling approach followed that used previously for SPP vadose-zone samples (Bond et al., 2008; SPP is a historic excavation where ERSP samples were obtained for research near IFRC well #3-26). Reasonable fits were obtained using reactions 1 and 2 (independently) in Table 1, with reaction 1 providing a significantly better fit as measured by the weighted sum of squares of the residuals divided by the degrees of freedom (WSOS/DF). Similar log K values for these reactions were obtained in single-reaction fits of adsorption data for the SPP vadose-zone samples (-4.43 and -0.27 for reactions 1 and 2, respectively, J. A. Davis, oral communication) but including both reactions 1 and 2 significantly improved the fit (Bond et al., 2008). Although the IFRC data obtained to date could not be fitted in any two-reaction model that included reaction 1, it is possible that data collected over the entire range of alkalinities applicable to the Hanford 300 area will require a two-reaction fit.

Additional experiments are underway to better constrain surface complexation model fits. Results of these experiments will span a much larger range of alkalinity values and adsorbed and dissolved U concentrations. Results of these further experiments will also allow SCM's to be obtained for each individual composite sample in order to quantify spatial variability in adsorption properties of sediments within the IFRC experimental domain. This first round of surface complexation constants is now being integrated into models used for interpretation of the three intact column experiments (Task 7), and for premodeling the planned October 2009 U desorption study (Task 6).

Table 1. Results from the three best-fit surface complexation models for the IFRC smear-zone composite sediment samples.

Number	Reaction(s)	logK	WSOS/DF
1	$SOH + UO_2^{2+} = UO_2OH + 2H^+$	-4.14	7.8
2	$SOH + UO_2^{2+} + H_2CO_3 = UO_2HCO_3 + 2H^+$	0.24	13.9

Hydrologic Characterization

Nothing to report.

Task 5. Vadose Zone Experimental Program

There has been no significant change to this task since the last report. Characterization data are continuing to be generated to quantify the unsaturated water transport properties of vadose zone sediments, and contaminant U concentrations in the vadose zone and capillary fringe that will enable more accurate planning of the vadose zone experimental site and associated research opportunities. Current plans call for development of the vadose zone site in FY10 after our mid-term project review.

EM-40 is preparing for a polyphosphate infiltration treatability study near the 300 A North Process Pond to evaluate the effectiveness of surface applied polyphosphate to reduce U fluxes to groundwater from the lower vadose zone during periods of high water table. The field site has been constructed, geologic characterization completed, and testing of the ERT system is underway. Geochemical laboratory experiments and vadose zone model construction have also been initiated to prepare for the infiltration test in August-September of FY 2010. The results of this EM study will likely influence the nature of vadose zone experimentation performed at the ERSP-IFRC site.

Task 6. Saturated Zone Experimental Program

August 09 Non-Reactive Tracer and Geophysics Experiment

A tracer experiment was performed in August 2009 to evaluate the electrical resistivity tomography (ERT) monitoring system and its ability to image tracer transport throughout the IFRC well field. It is expected that this system will be used to monitor the dynamic behavior of future injection experiments and to provide real-time measures of mass transfer to or from fine-

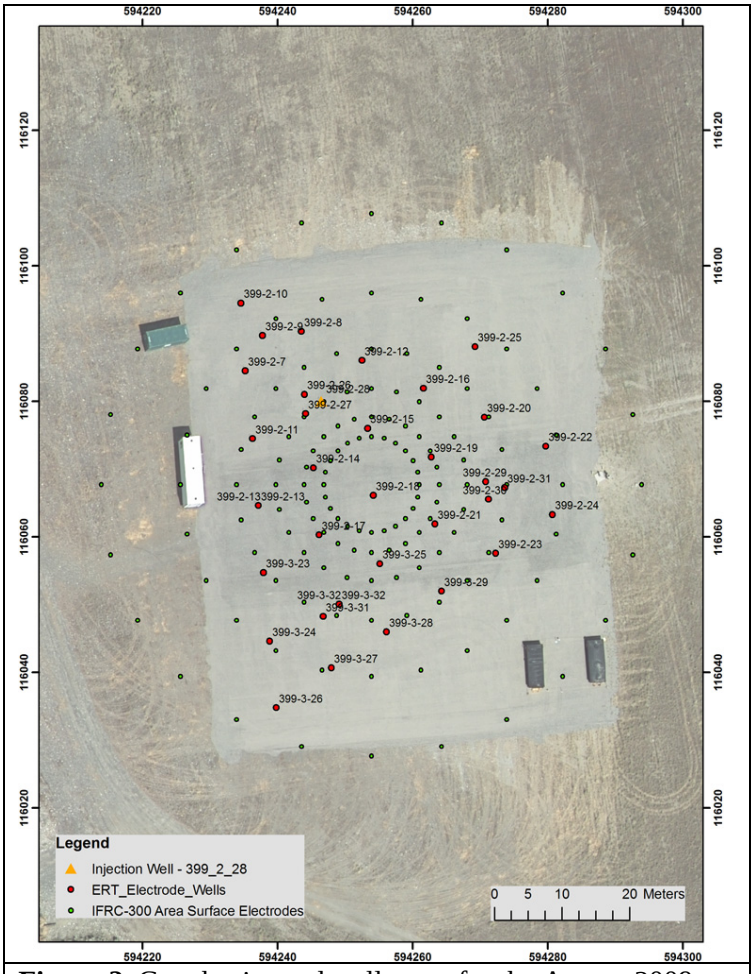

Figure 2. Geophysics and well array for the August 2009 small-scale injection experiment.

grained domains. Consequently, test design focused on approaches having the greatest potential for creating a tracer plume of appropriate size, geometry, and electrical/transport characteristics for effective ERT imaging.

The resulting experimental design involved injection of a conservative tracer into a single intermediate zone well (399-2-28, Figure 2) that was completed over a depth interval comprised of intermediate to relatively low permeability materials that is both over and underlain by higher permeability materials. This approach was based on an assumption that the tracer mass could be contained largely within the lower permeability zone and not escape to the over and underlying more permeable zones during the injection phase. The experiment was expected to result in an adequately sized, relatively slow moving tracer plume well suited to ERT imaging. Although depth discrete aqueous monitoring locations available to support the primary objectives of this experiment were limited to the injection well and the upper and lower zone wells at this location, this single three-well cluster and adjacent fully screened wells did provide a means for assessing both escape of tracer from the targeted zone during the injection phase and elution of tracer from the targeted zone during the drift phase of the experiment. It was estimated based on available geohydrologic characterization data and simplified volumetric calculations that up to 30,000 gallons of tracer solution, resulting in a plume radius of ~10 m, would be injected during the experiment.

A new electrode array geometry was deployed during this injection experiment to allow for more rapid measurements than could be realized using the ERT well electrodes alone. The new array included 169 surface electrodes arranged in concentric circles with telescoping radii (Figure 2 and 3) and 48 non-polarizable reference cells (Cu-$CuSO_4$) at alternate locations. Interrogation of the surface electrodes using mise-a-la-masse (MALM) methods required only 4 minutes, whereas interrogation with a gradient array geometry required 5 hours. Self Potential (SP) measurements with the 48 non-polarizable reference cells required only 1 minute to complete. The most frequent and rapid monitoring during the injection experiment used combinations of these surface and subsurface electrodes.

The ERT well electrode geometry (Figure 3) and the MPT-DAS1 operating system were optimized to acquire data as rapidly as possible in order to capture dynamics of the tracer experiment. ERT surveys as previously deployed at IFRC require several days to complete. ERT measurement time was reduced by measuring only groundwater level

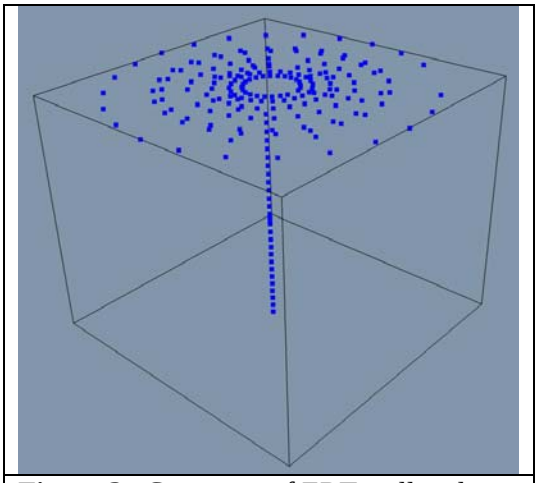

Figure 3. Geometry of ERT well and surface electrodes.

electrodes, reducing the complexity of the array geometry, eliminating reciprocal measurements and increasing the base frequency of the MPT-DAS1. Using this configuration allowed for 29 minute measurement times over 8 well clusters. Well clusters were initially focused around the injection well and then expanded to the entire well field over time.

A solution containing a conservative tracer (~480 mg/L Br^-) was injected at a constant rate into well 399-2-28. The tracer solution was injected for 1057 min (~17.6 hrs) at an average rate of 20.4 gpm, for a total injection volume of 21,550 gal. Operational procedures called for injection stream samples to be collected from within the injection well screen using a submersible pump. However, due to interference with the electrical connections of the ERT systems, this approach had to be abandoned and the injection manifold modified to allow for injection stream sample collection. It is expected that the down well SpC data provide a more accurate measure of the level of injection concentration variability during the injection phase than that indicated by the IC data.

The test was run until it became apparent that tracer was escaping from the targeted zone and being transported down gradient, at which time the injection was stopped and the tracer plume was allowed to drift under natural gradient conditions. During the drift phase, tracer was monitored in the injection well (Figure 4) to assess tracer elution from the targeted lower permeability interval, and in fully screened wells throughout the well field to assess transport through the more permeable regions of the aquifer. In addition to aqueous sample collection, the plume was tracked by monitoring specific conductivity with down well probes and through ERT measurements.

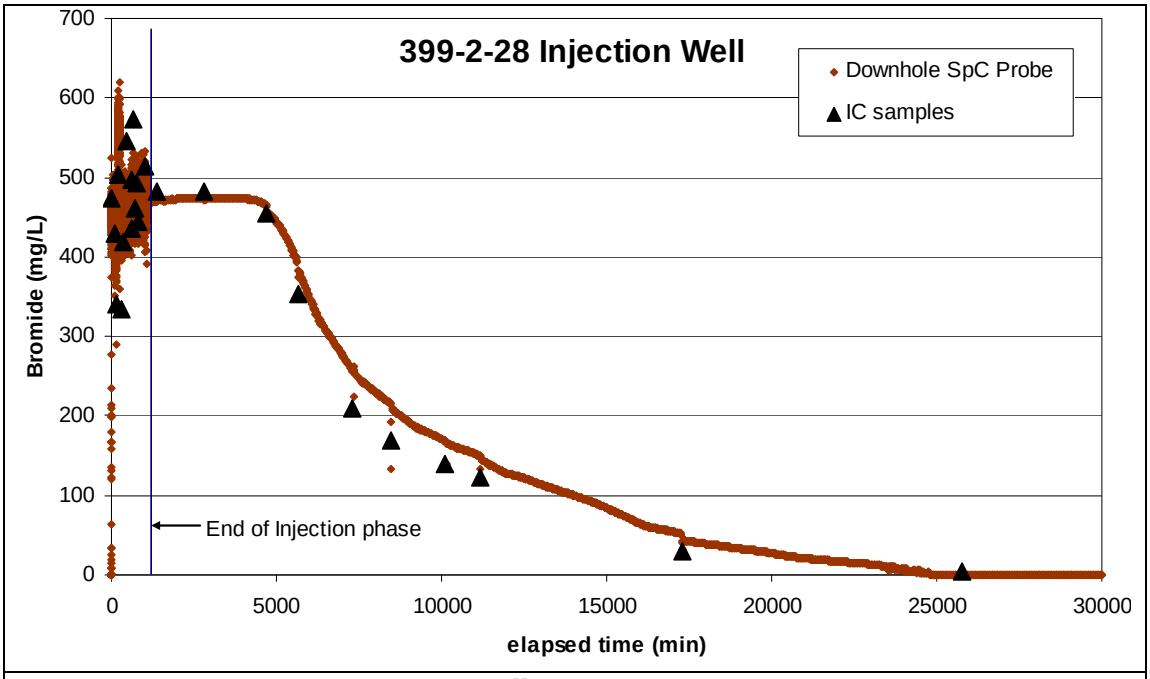

Figure 4. Tracer response in injection well 399-2-28.

During all phases of the experiment, no tracer was observed in the adjacent upper and lower zone wells, indicating that a significant amount of the tracer mass was injected into the lower permeability zone. However, tracer was observed in fully screened wells along the preferential flow channel identified during the March experiment (Figure 5; 2-18, 3-29). This observation indicated that some tracer mass was released to the higher permeability materials and was transported through this channel, likely along a relatively thin zone just above or below the lower permeability materials (potentially thicker in the lower zone due to density sinking). Continuous specific conductance measurements in

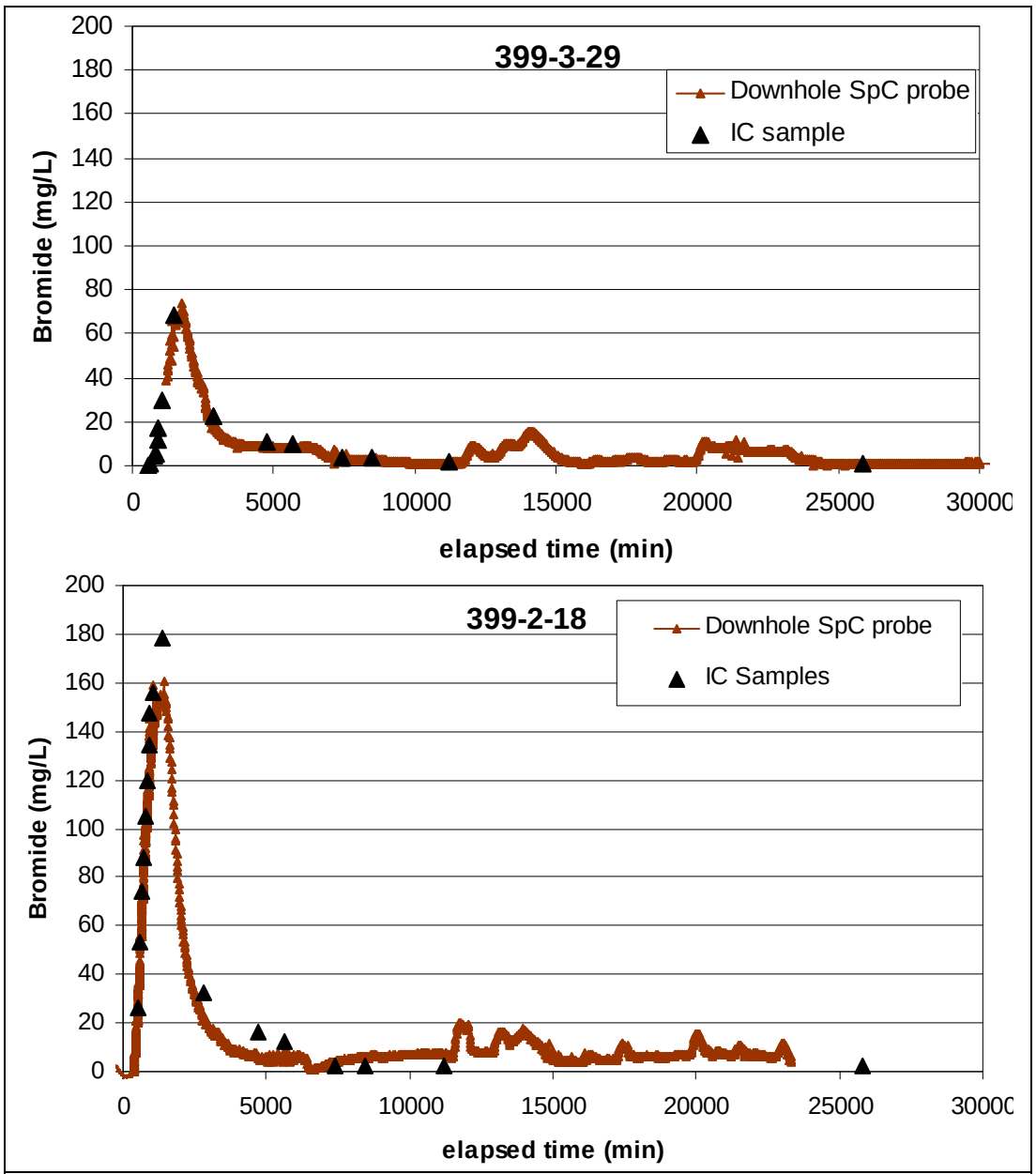

Figure 5. Tracer arrival and elution response at selected down gradient well locations.

well 399-2-18 indicate that initial tracer arrival was observed approximately 500 minutes into the test, with tracer concentrations reaching 30% of the injection concentration after 1000 minutes (Figure 5). Well 399-3-29, located at the down-gradient end of the well field, saw initial arrival near the end of the injection phase, indicating that most of the tracer mass was retained within the well field. The rapid elution response in down gradient monitoring wells implies that once injection was ceased, transport of tracer out of the lower permeability zone decreased significantly.

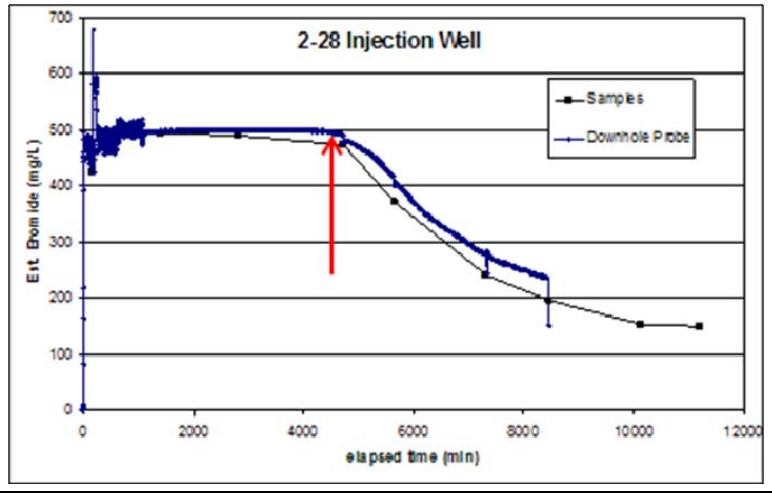

Figure 6. Post injection gradient array sampling time (red arrow).

Gradient array resistivity data was acquired (5 hour acquisition time) from 169 surface electrodes in July, and just after the injection experiment (Figures 6 and 7). Injection pumps were not energized during these surveys. Low resistivity contours from 1-25 ohm-m in Figure 7 were chosen in order to focus on temporal changes in resistivity related to the 9 ohm-m tracer injection. A low resistivity plume-like feature (red circle) persists around the injection well after 76 hr, 4560 min (Figure 7). This low resistivity

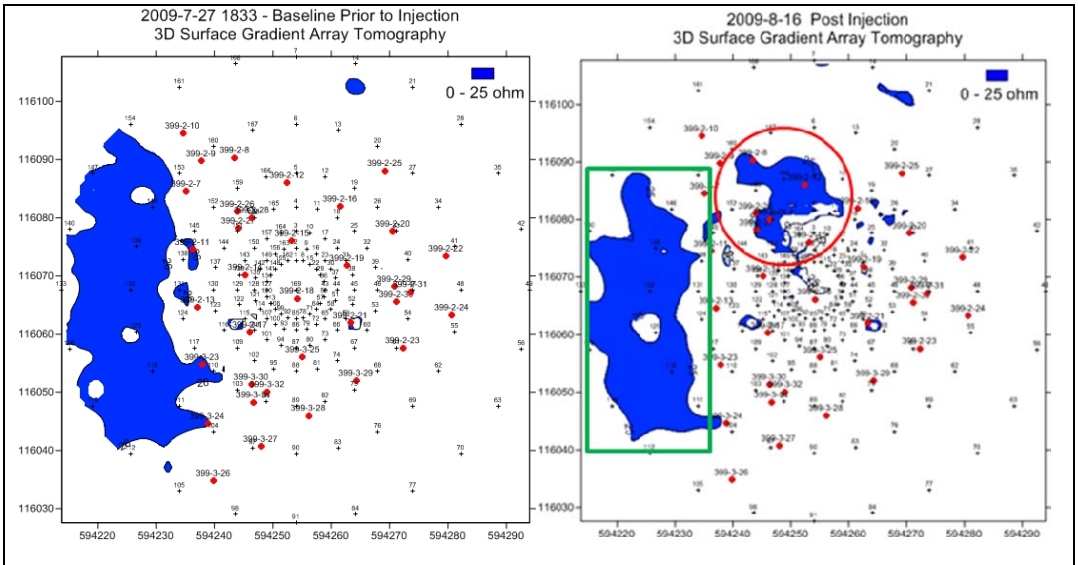

Figure 7. Comparison of baseline vs. post injection gradient array data. Pump motors were not energized during these surveys. The red circle indicates new low resistivity feature centered around injection well. The green box indicates a low resistivity trench feature (also imaged with prior EM and two-dimensional resistivity surveys).

target coincides with direct samples of tracer in the injection well after 3 days (4320 min). A second low resistivity target is located along a western trench like feature (green rectangle). This trench like feature was visualized during previous electro-magnetic (EM) and two-dimensional resistivity surveys, and is characteristic of the subsurface at this location.

ERT data over the entire well field was collected after the injection experiment was completed on all 840 vadose zone and groundwater well electrodes in the same manner as deployed for electrical facies mapping. These higher resolution and longer running measurements target the residual tracer which may remain long enough to be imaged with ERT. These measurements include full reciprocals for error and noise analysis resulting in 90.5 hours of collection time and approximately 281,350 measurements. The MPT DAS-1 ERT systems current configuration (8 channels and 256 multiplexed switches) is maximized by running 5 separate sets of 8 well clusters to measure all 30 wells at IFRC. Each 8 well cluster takes 18.1 hours to complete and requires system checks and manual switching before moving to the next well cluster. A full 840 electrode

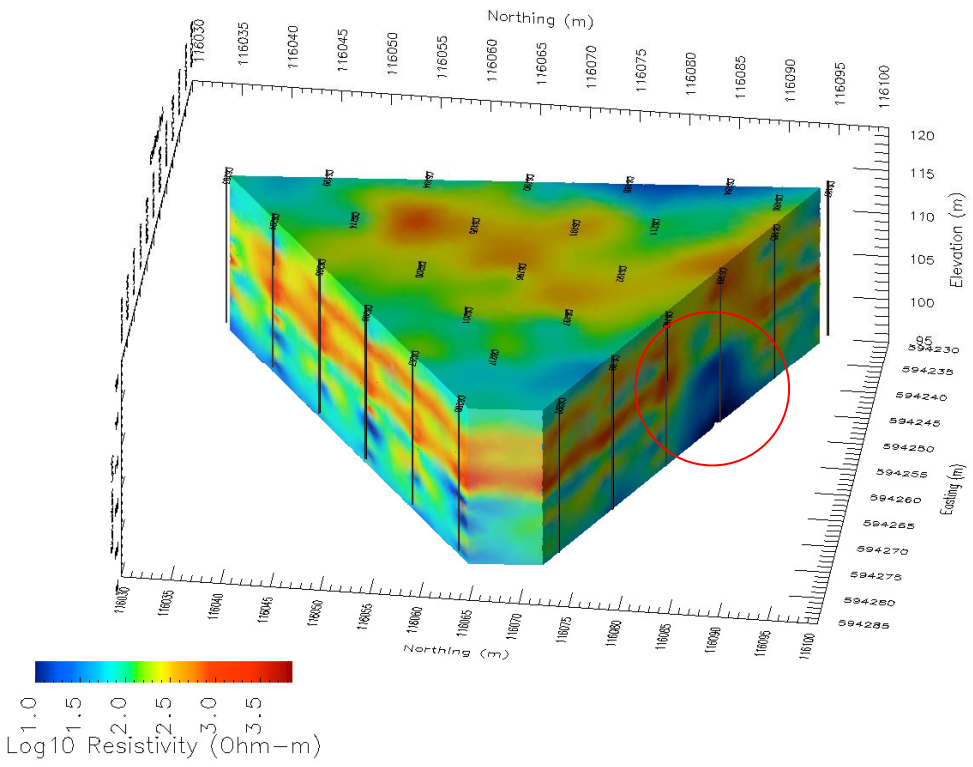

Figure 8. Preliminary ERT FERM3D L2-norm inversion model (840 electrodes over 30 wells). View is from above and east of the IFRC well field. Note the low resistivity feature in the water table and vadose zone near injection well (C6205/399-3-28) that trends above and to the north-east of the injection point.

ERT survey is currently being processed with both the FERM3D (INL) and Res3DINVx64 inverse model codes. Preliminary inversion results are shown in Figures 8 and 9. Physical retardation in the low K zone, and apparently discontinuous migration in the higher K regions is evident. This first attempt at dynamic plume monitoring shows the potential power of this technique. Data analysis is continuing on the many geophysical and water compositional measurements performed during this experiment.

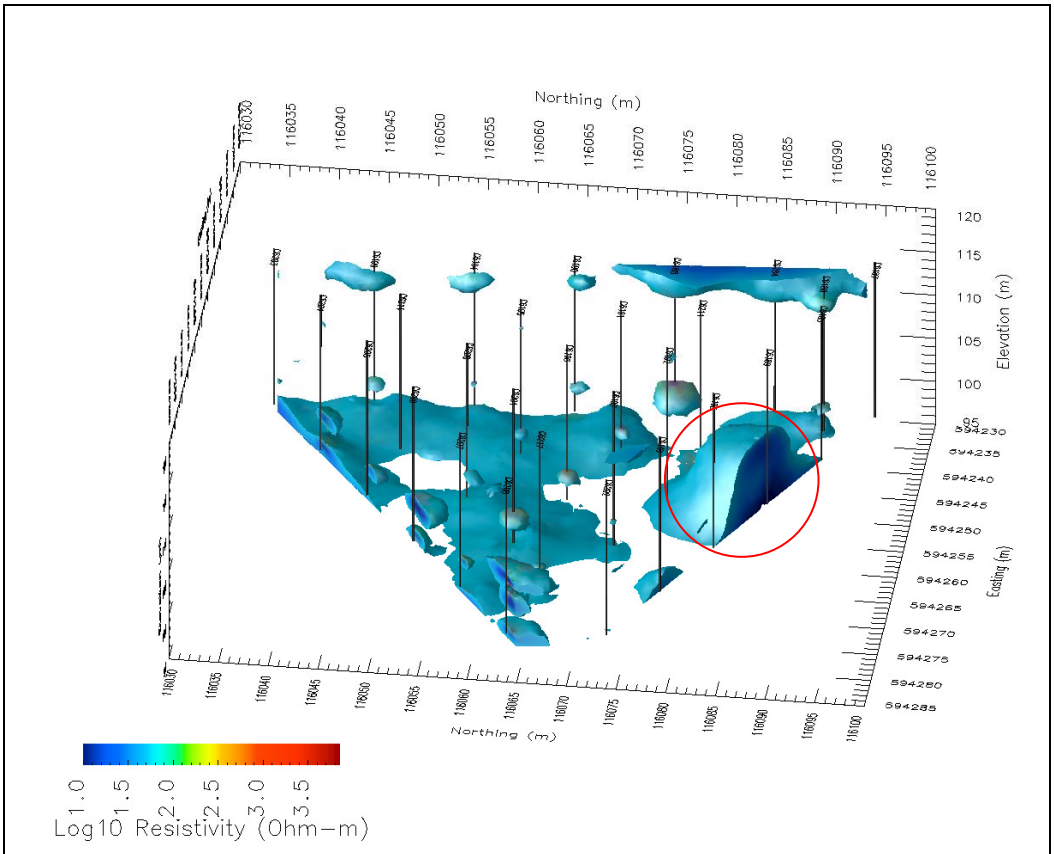

Figure 9. Preliminary ERT FERM3D L2-norm inversion model (840 electrodes over 30 wells). View is from above and east of the IFRC well field with higher resistivity values masked. Note the low resistivity feature in the water table and vadose zone near injection well (C6205 / 399-3-28) that trends above and to the north-east of the injection point.

Additional FY 09 Field Experimental Plans

A warm month, low river stage (October 2009) reactive transport experiment is planned where up-gradient groundwater with lower U(VI) concentration (approximately 6 ppb) will be injected in the IFRC site where current U(VI) concentrations are 60 ppb. The plume will be monitored during transport to assess in-situ U(VI) desorption and mass transfer kinetics, and their linkage to previously characterized flowpath and lithologic heterogeneities in the March 2009 experiment. Final source well selection is underway

with 399-1-15 being the primary candidate with two backup wells identified (399-1-14A and 399-1-6). Isotopic analyses are being performed on samples from all three wells. The experiment will inject two, sequential 50,000 gallon tracer clouds to create a more extended plume for investigation of in-situ desorption kinetics.

Task 7. Modeling and Interpretational Program

Progress Summary for the Modeling Team

The modeling team has been focused on three primary activity areas.

1. Establishing a robust model for the distribution of hydraulic conductivity and related properties/parameters for the IFRC field site by integrated analysis and inversion of various data sets, including electromagnetic borehole flow-meter surveys, tracer experiment results, laboratory grain size and other analyses of borehole sediments, and down-hole geophysical measurements (Geophysics Inversion and MAD Progress).
2. Developing a detailed IFRC site hydrologic model through integration of the field hydrologic and geophysical characterization results; modeling of the first three non-reactive tracer experiments, including the non-isothermal experiment; and simulation of continuous temperature, electrical conductivity, and well head responses of the IFRC well field to Columbia River stage changes during the passive spring experiment (Hydrologic Model Development).
3. Parameterizing a geochemical model (for eventual field site application) that accurately and realistically describes the kinetic adsorption/desorption process currently attributed to mass transfer by modeling U(VI) desorption and adsorption behavior measured in various large-scale and intact laboratory columns of IFRC site sediments. Different modeling approaches (PFLOTRAN, STOMP) are being used to identify the most versatile, yet realistic and robust approach for field application (Reactive Transport Model Development and Field Scale Reactive Transport).

Geophysics Inversion

ERT data collected earlier in 2009 were evaluated with an inverse operation to determine the electrical conductivity distribution of the IFRC well field. This was done by minimizing the difference between observed data (D_{obs}) and calculated data (D_{cal}) associated with a specific model. This minimization was done by changing the model with constraints placed on the solution so that the problem is well posed. Typically these constraints come in the form of minimum structure, meaning that the only heterogeneity in the inverse solution is that which is resolved by the resistivity measurements. This

results in a smoothed image of the actual conductivity structure.

There are multiple conductivity models which are equally acceptable from a difference perspective. However, the goal is to find a model of electrical properties which approximates the true distribution. To do this, there are several possible methods including coupled or joint inversion and use of geostatistics, which was deployed for inverting the ERT measurements. The solution must honor both the resistivity measurements and the geostatistical structure defined by one or more semivariograms.

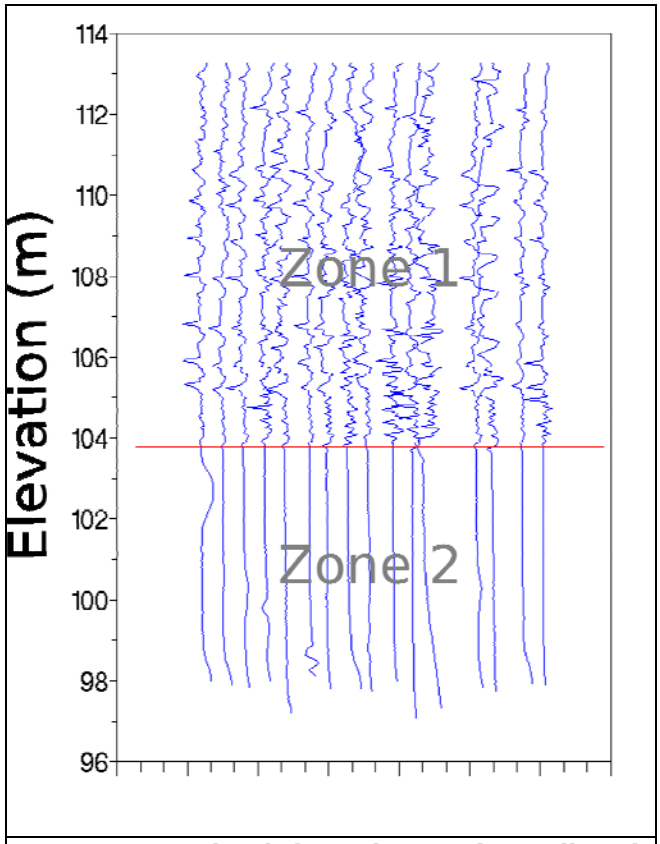

Figure 10. EM borehole conductivity logs collected in the IFRC well field. The logs suggest two zones with differing electrical conductivity structures. These correspond to the vadose zone and the saturated zone.

The electrical conductivity semivariograms were estimated using borehole conductivity measurements collected in 18 of the IFRC wells (Figure 10). For geostatistical analysis, the well field was divided into two zones with different geostatistical structures as indicated by the logs, as determined by the location of the water table. Data from each zone were used to approximate the horizontal and vertical semivariograms, which were, in turn, used to constrain the ERT inversion in each zone. These logs provide detailed conductivity information along the length of the borehole, but are spaced approximately 10 m apart within the IFRC well field. Therefore, variance estimates are detailed in the vertical direction, but may only be computed at 10 meter intervals in the horizontal direction.

Zonal semivariograms were estimated from the borehole logs shown in Figures 10 and 11. The colored dots show the horizontal experimental semivariograms for each zone in each of the three directions along which wells are aligned. Note there is no obvious anisotropy in the horizontal range, so we use a single horizontal semivariogram for each. The black dots show the vertical experimental semivariogram for each zone. The magenta lines show the horizontal model semivariogram which we use to constrain the inversion, and the black lines show the corresponding vertical semivariograms. The sill values are equivalent in each zone.

Inverse solutions resulting from a minimum structure approach and a semi-variogram constrained approach show significant differences (Figure 12). The minimum structure constraints specify zero first order spatial derivatives with a weight of 10 horizontal to 1 vertical, which enhances horizontal continuity (i.e. provides a layered solution). Note the minimum structure inversion appears to be a smoothed or smeared version of the semivariogram-constrained inversion. The semivariogram-constrained inversion appears to delineate smaller scale features which the resistivity data alone cannot resolve. While it is likely these smaller scale features exist, this can only be validated with the uncertainty analysis described above.

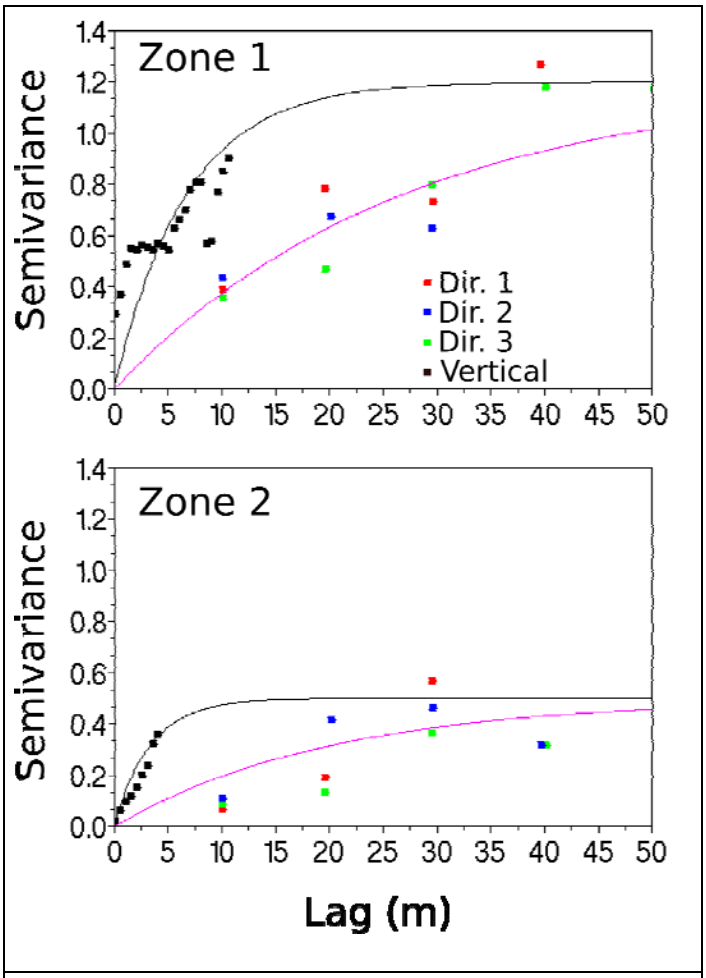

Figure 11. Experimental and model semivariograms for each zone. The colored dots indicate the horizontal variance in the three directions in which wells are primarily aligned. The black dots indicate the corresponding vertical variance for each zone. The magenta lines show the horizontal model semivariograms chosen to constrain the inversion. The black lines show the corresponding vertical semivariograms**.**

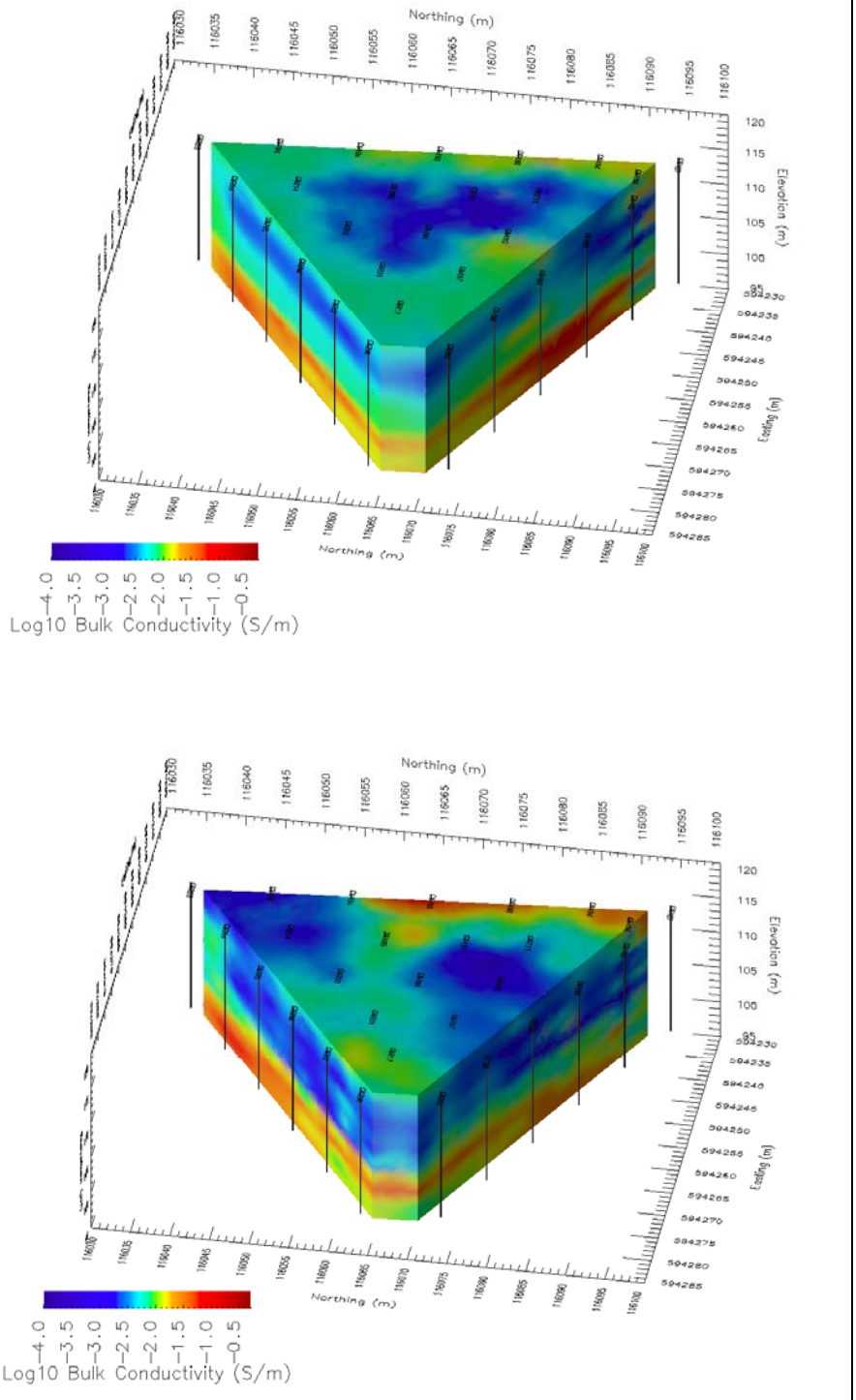

Figure 12. Minimum structure inverse solution (top) and semivariogram constrained inverse solution (bottom).

MAD Progress

The UC Berkeley team working on developing the Method of Anchored Distributions (MAD) made progress on several fronts. They continued development of the inverse modeling platform based on the concept of anchored distributions and applied the platform to data collected at the IFRC 300 field site; developed a detailed, fine-grid characterization of the field site based on IFRC's pump tests and electronic bore flowmeter (EBF) data; and initiated analysis of the March 2009 transport experiments. A summary of these items is provided below.

Development of the inverse modeling platform

The development of the inverse modeling platform included extensive testing of MAD using synthetic studies, and an investigation of anchor placement strategies. Testing of MAD was done with interpretation of data obtained from synthetic data fields that mimic the geological conditions and data acquisition strategies at the 300 Area IFRC. These analyses gave confidence in MAD and in its ability to interpret correctly the actual field data. The anchors are the key for data assimilation. However, there is a strong incentive, in terms of computational effort, to minimize the number of anchors employed. The team is working on developing a strategy to optimize the number of anchors employed for inverse modeling.

Fine-grid characterization based on pumping tests and EBF data

The MAD inverse platform was applied to the IFRC pumping tests and electronic borehole flowmeter (EBF) data with the goal of generating high-resolution, three-dimensional distributions of the hydraulic conductivity at the field site. A multi-step approach was used. In the first step, the pump tests were interpreted based on the spatial distribution of transmissivity (Figure 13). The transmissivity values obtained at the wells were then converted to vertical profiles of the conductivity based on the EBF data and were used to estimate a 3D geostatistical model of the field. Finally, the geostatistical model was used to generate 3D realizations of the conductivity field (Figure 14). These data are being provided to the other IFRC modeling groups.

Analysis of transport experiments

The MAD team started analyzing the March 2009 transport experiment with a goal to use the experimental data for further conditioning of the hydraulic conductivity fields. These data will be interpreted by coupling MAD with a numerical flow and transport simulator.

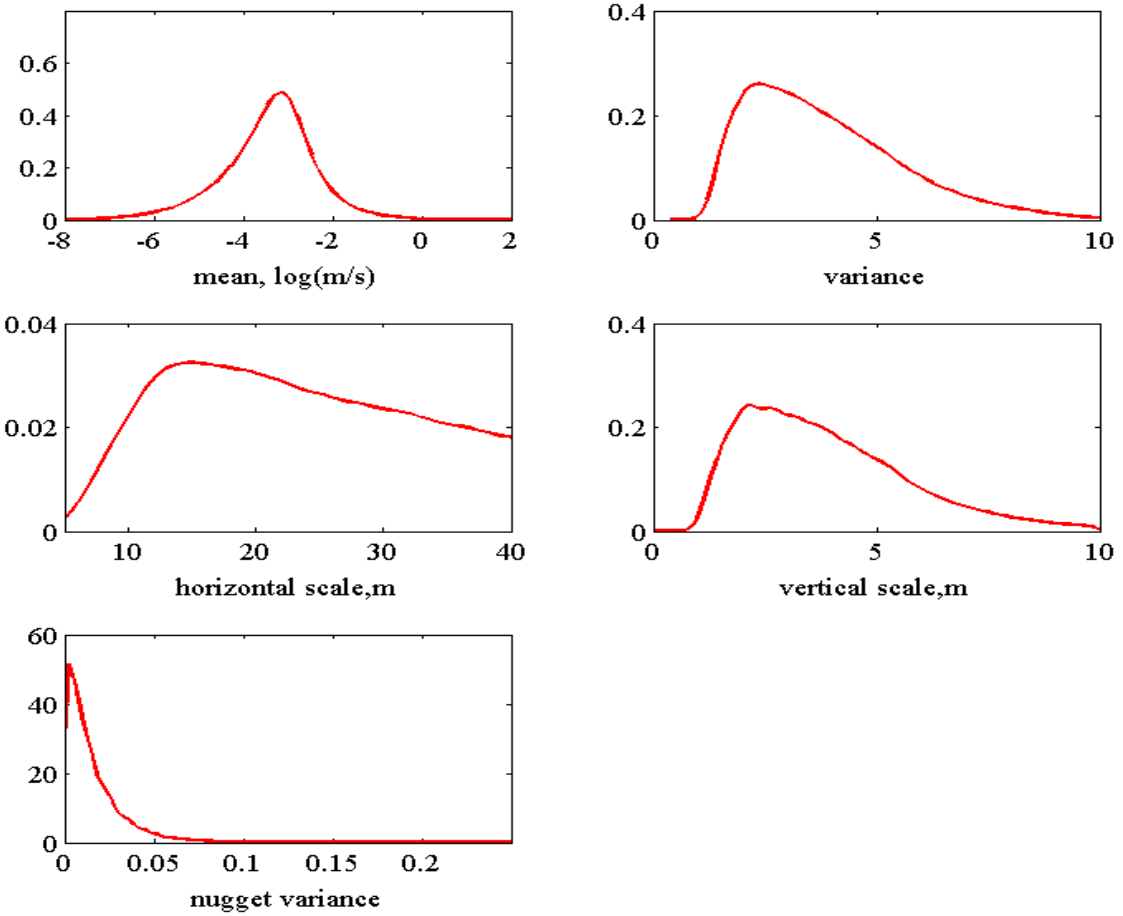

Figure 13. Statistical distributions of the geostatistical parameters of the Hanford IFRC 300 site. This plots show the distribution of the mean Ln(K) field, and the distribution of the spatial covariance of Ln(K), including the variance, the nugget, the horizontal integral scale and the vertical one.

toward that goal, MAD is being linked with PFLOTRAN and the codes modified to run on Franklin, the NERSC supercomputer.

To establish a benchmark for the MAD/PFLOTRAN analysis, and in order to guide understanding of the dominant processes controlling flow and transport at the IFRC site, interpretation of the field data was initiated using simplified analytical models. The simplified analytical models were found to yield adequate interpretations of the field data.

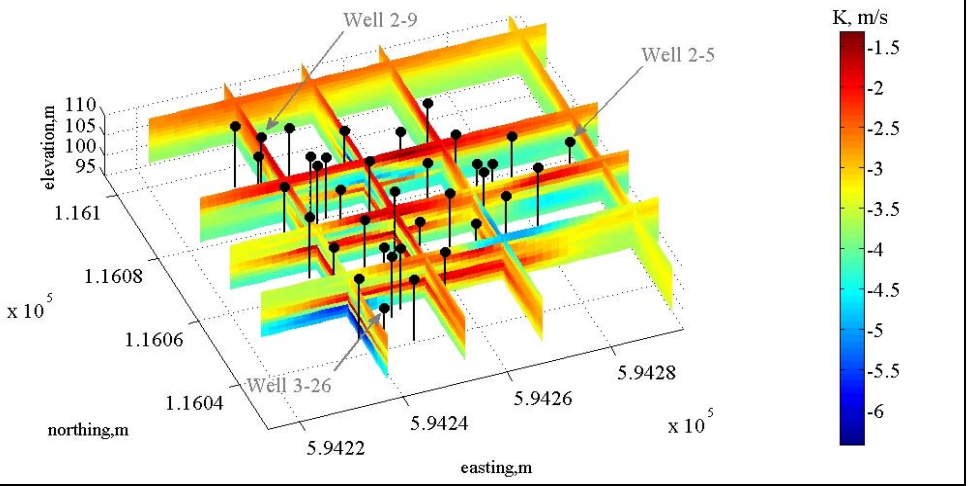

Figure 14. A three-dimensional image of the mean Ln(K) field at the Hanford IFRC 300 site. The color scale is for the Ln(K), with K in m/s.

IFRC Hydrologic Model Development

The conservative tracer and heat transport experiments conducted at the IFRC site in November 2008 and March 2009 have been simulated with MODFLOW and STOMP. The previous quarterly report included results of tracer experiment simulations with STOMP. A parallel effort has been made with MODFLOW by the University of Alabama team. The three-dimensional IFRC plot-scale flow and tracer transport models based on MODFLOW reproduce the observed bromide (Br) tracer plums for both 2008 and 2009 tests (Figure 15 shows a comparison of observed and simulated bromide breakthrough curves at an observation well during the March 2009 experiment). The next step will be to incorporate more detailed hydraulic conductivity distributions from the inverse modeling efforts and incorporate them into the flow and transport model. New approaches are being explored to handle the complex and highly transient Columbia River boundary conditions more effectively.

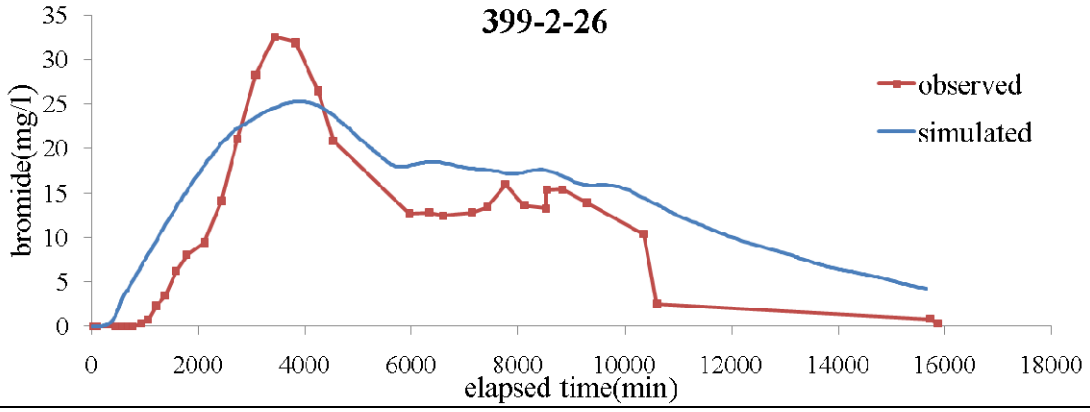

Figure 15. Comparison of observed and simulated bromide concentrations at observation well 399-2-26 based on preliminary simulation analysis of the March 2009 tracer experiment.

The University of Alabama team has also been evaluating the use of temperature data in combination with Br tracer data to quantify the three-dimensional hydraulic conductivity distribution at the IFRC site using the heat tracer data from the March 2009 experiment. Groundwater flow simulation was carried out with the MODFLOW code, while heat tracer transport simulation was conducted with the MT3DMS code under the assumption of constant fluid density and viscosity. The inverse code PEST was employed to help calibrate the flow and transport models. The simulation results show that the groundwater head data alone are insufficient to constrain the hydraulic conductivity distribution, especially because the Hanford formation is highly permeable with the hydraulic conductivity in the range of 7000 m/day. While the Br tracer data are very important to improving the estimation of hydraulic conductivity, continuous Br data in 3D are expensive to acquire. The temperature data can be a cost-effective proxy for conservative solute tracers such as Br.

Reactive Transport Model Development

Efforts have been focused on development of both laboratory and field-scale reactive transport models.

Parameterization of a reactive transport model

Reactive transport experiments have now been completed with three intact cores from the IFRC saturated zone. The individual core sections were selected to represent the three prominent facies types that our characterization measurements have shown to be present in the IFRC domain. All three columns/cores showed very comparable behavior, and, for that reason, only one will be discussed here. The absence of significant differences between the three cores was a good

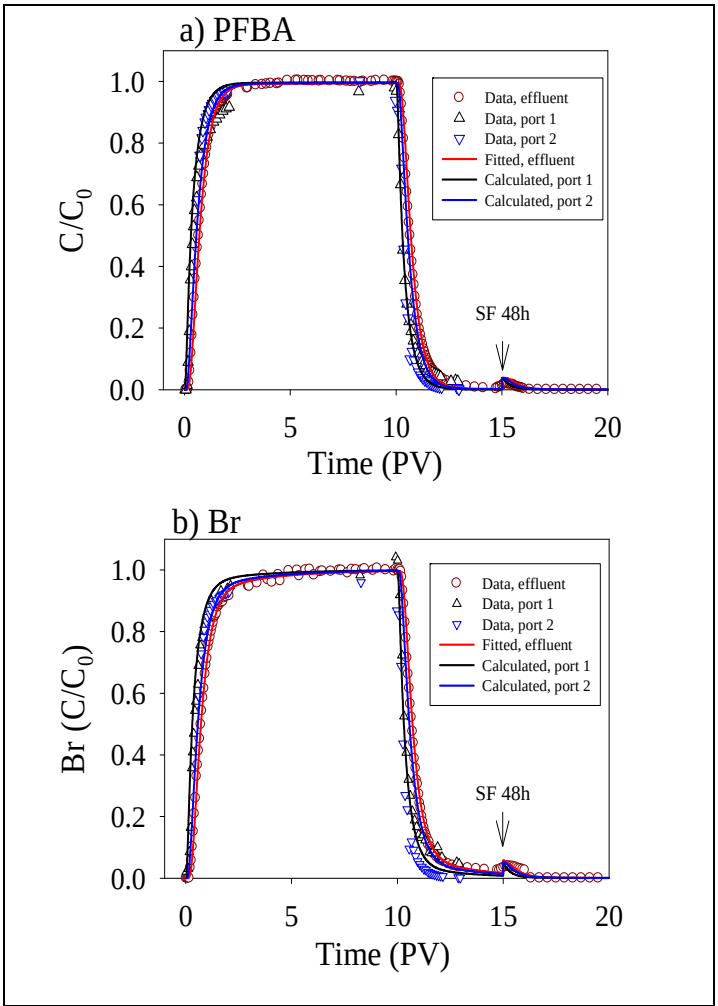

Figure 16. Measured and modeled breakthrough curves of PFBA (plot a) and Br (plot b) for Phase B of column ICE-1. SF denotes stop-flow event with SF duration noted in the plots. Sampling port 1and 2 are 1/3 and 2/3 of the column length from the flow inlet end of the column, respectively.

finding in that it implies that the reactive transport properties of the saturated zone are relatively homogeneous. Reactive transport parameters derived from these intact column experiments will be used to pre-model our first reactive transport experiment with U(VI) in October 2009.

The experiments were run with three phases: A – desorption of in-situ contaminant U(VI), B – transport of non-reactive tracers (Br and PFBA) with continued contaminant U(VI) desorption, and C – adsorption and desorption of a 60 ppb U(VI) pulse (Figures 16 and 17). Qualitatively, the core experiments revealed rapid breakthrough through preferential flow-paths created during core collection, and strong retardation to fines that were a minor physical component of the sediment. The tracer (Br and PFBA) and U effluent data were modeled using a dual-domain, adsorption(surface complexation)-retarded, kinetic 1D reactive transport model (Liu et al., 2008). This model provided a good description of the non-reactive tracer behavior (Figure 16) with the model parameters provided in Table 2. The estimated mass transfer coefficient (ω) for Br was larger than that for PFBA. This was consistent with a diffusion mechanism as the control of mass exchange between the mobile and immobile domains. Diffusive mass exchange was predicted to be faster for a species with a larger diffusion coefficient (Br) than for a species with a smaller diffusion coefficient (PFBA). The molecular diffusion coefficient ratio of Br versus PFBA is 2.67. The estimated ratio of the mass transfer coefficients of Br versus PFBA was 8.13, indicating that the mass transfer coefficient of a species was not simply scaled to its molecular diffusion coefficient.

Table 2. Parameters used in modeling tracers and U(VI) adsorption/desorption for ICE 1.

Pore water velocity, v	10.36	cm/h	measured
Total porosity, θ	0.30		measured
Dispersion coefficient, D	55.2	cm^2/h	PFBA and Br effluent
Mobile porosity, θ_m	0.24		PFBA and Br effluent
Immobile porosity, θ_{im}	0.06		PFBA and Br effluent
Mass transfer coefficient, ω	$1.82x10^{-2}$	h^{-1}	PFBA effluent
	$1.48x10^{-1}$	h^{-1}	Br effluent
Sediment bulk density, ρ_b	1.91	kg/L	independent estimate
<2 mm size mass fraction	24.7%		independent estimate
<2 mm size bulk density, ρ^f_b	0.47	kg/L	independent estimate
Labile U(VI) in < 2mm size fraction	454.2	ug/kg	independent estimate
U distribution coefficient, K_d	15.5	mL/g	from U desorption
Logarithm mean of rate constant, μ	-6.62	$\log(h^{-1})$	from U desorption
Deviation of log rate constant, σ	2.69	$\log(h^{-1})$	from U desorption

The model well described the ICE-1 effluent U(VI) in all phases (Figure 17) with the same set of the parameters. In that model, the < 2mm size fraction was assumed to be the

only solid reactive fraction that was distributed between domains with mobile and immobile water. The model further assumed that uranium desorption in the immobile domain required a two step mass transfer processes: from the <2 mm solid to aqueous phase in the immobile domain, and from the immobile aqueous to mobile aqueous domains. The U(VI) desorption in the mobile domain only required the mass transfer from the < 2 mm solid to aqueous phase. The adsorption in both the mobile and immobile domains was the reverse of the desorption processes. The mass exchange rate of aqueous U(VI) between mobile and immobile phases was described using a multiple first-order rate expression with respect to the deviation of U(VI) adsorption from its equilibrium state. The adsorption equilibrium state was described using a surface complexation model. However, the surface complexation model for these core sediments has not been established. Here a K_d-based model was used to approximate the surface complexation model by assuming that the adsorption/desorption isotherm was linear, and solution chemical composition was constant during the column experiments. The fitted K_d was unexpectedly large (e.g., 15.5 mL/g), attesting to the strong adsorption affinity of the fines. A surface complexation model will be parameterized for these particular sediments in FY 10 based on the approach described in Task 4 (above) that will be integrated into our evolving site reactive transport model.

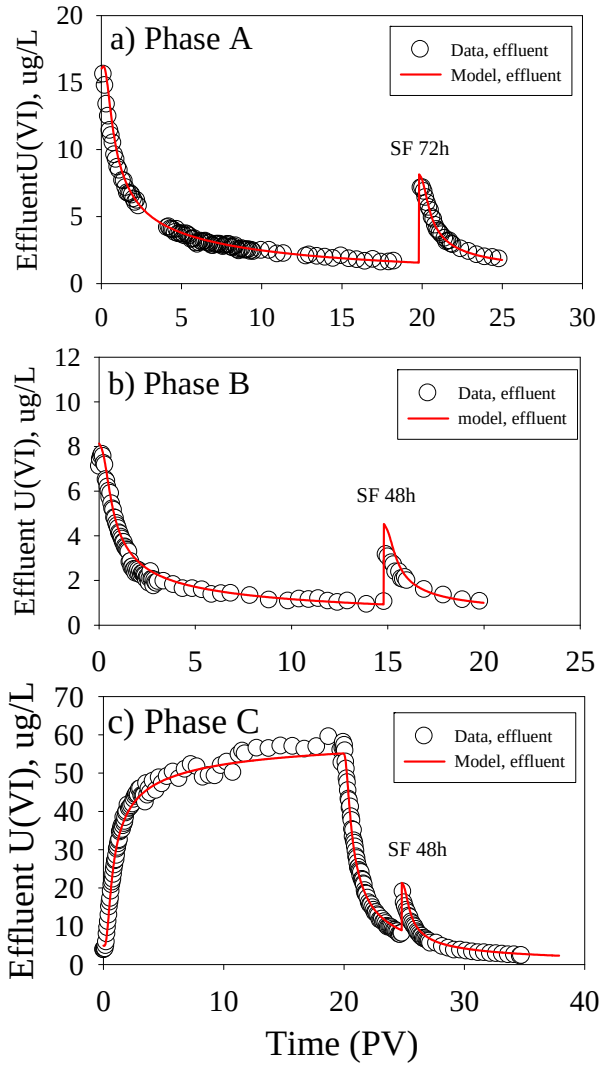

Figure 17. Measured and modeled breakthrough curves of U(VI) in desorption phase A (plot a), tracer breakthrough with desorption phase B (plot b), and adsorption/desorption phase C (plot c) in column ICE-1. Data in phase A was used to fit the U(VI) mass transfer parameters in the sediment. The mass transfer model with the fitted parameters was then used to predict the effluent U(VI) in phases B and C.

Field-Scale Reactive Transport

U(VI) migration influenced by coupled multi-rate mass transfer and surface complexation reactions

The University of Alabama team has developed a two-dimensional cross-sectional reactive transport model through the 300A IFRC site (Figure 18). The cross-sectional model has the eastern boundary at the Columbia River to account for changes in aqueous chemistry from mixing of river water and groundwater. Measured hourly water levels in well 399-3-19 and at river gage SWS-1 were used for the prescribed piezometric head boundary conditions at the western end of the model domain and for the river boundary at the eastern end, respectively. To account for the full complexity of the uranium transport processes observed at the 300A site, equilibrium surface complexation reactions (SCR) and a new multi-rate SCR model developed by Liu et al. (2008) were used and compared to each other. The modeling study was intended to assess the importance of multi-rate mass transfer processes on the fate and mobility of uranium at the 300A IFRC site and to prepare for the planned uranium field experiments and subsequent modeling analyses beginning in October 2009.

The model simulations revealed complex spatio-temporal relationships between groundwater composition and U(VI) speciation, adsorption, and plume migration. In general, river water intrusion enhances uranium adsorption and lowers aqueous uranium concentration, as river water dilution increases pH and decreases aqueous bicarbonate concentration, leading to overall enhanced U(VI) surface complexation. Strong U(VI) retardation was computed for the field-measured hydrogeochemical conditions, suggesting a slow dissipation of the U(VI) plume, a phenomenon consistent with field observations. The simulations also showed that SCR-retarded U(VI) migration becomes more dynamic and synchronous with the groundwater flow field when multi-rate mass transfer processes are involved. Breakthrough curves at selected locations and the temporal changes in calculated U(VI) mass over the 20-year simulation period indicated that uranium adsorption/desorption never attained steady state (e.g., equilibrium) because of the dynamic flow field and groundwater composition variations caused by river water intrusion. Thus, the multi-rate SCR model appears to be a crucial consideration for future reactive transport simulations of uranium contaminants at the 300A site and elsewhere under similar hydrogeochemical conditions.

Comparison of parameter sensitivities between a laboratory and a field scale model of U(VI) transport in a dual-domain, distributed-rate reactive system

Important scale related issues must be considered to apply the laboratory-derived, multi-rate SCR model (MR-DD-SCR) described by Table 1 (and as applied to Figures 16 and

17) to the IFRC field domain for U(VI) reactive transport calculations. These up-scaling issues are being addressed through a number of activities. A first step has been the performance of a rigorous sensitivity analysis of the laboratory model for various scenarios that incorporate the characteristic hydrological and hydrogeochemical conditions found at the IFRC site. The underlying conceptual and numerical model, originally developed from column experiment data, includes distributed-rate surface complexation kinetics of U(VI) to mineral surfaces, aqueous speciation, and physical non-equilibrium transport processes. The field-scenarios for sensitivity analyses accounted for highly transient groundwater flow and its effect on reaction timescales, and variable geochemical conditions driven by frequent water level changes of the Columbia River.

The sensitivity analysis unexpectedly revealed that parameter sensitivities were largely similar between the laboratory and field scale systems (Figure 19). However, important differences were also found because of the highly constrained conditions (e.g., constant flow rate and aqueous chemical composition) under which the laboratory experiments were performed. The MR-DD-SCR will be tested to its limits in the field where rapid changes in: i.) groundwater flow directions and head, and ii.) groundwater composition, cause transient, non-equilibrium adsorption/desorption events. Moreover, the calculation of in-situ concentrations near the plume margins are highly sensitive to a number of variables because of the low mass of U(VI) involved. This study has provided important insights on key variables controlling U(VI) transport under “in-situ” hydrogeologic conditions that will improve our characterization strategy for IFRC site sediments, and monitoring methodologies for U(VI) field experiments. Results are now being written-up for publication.

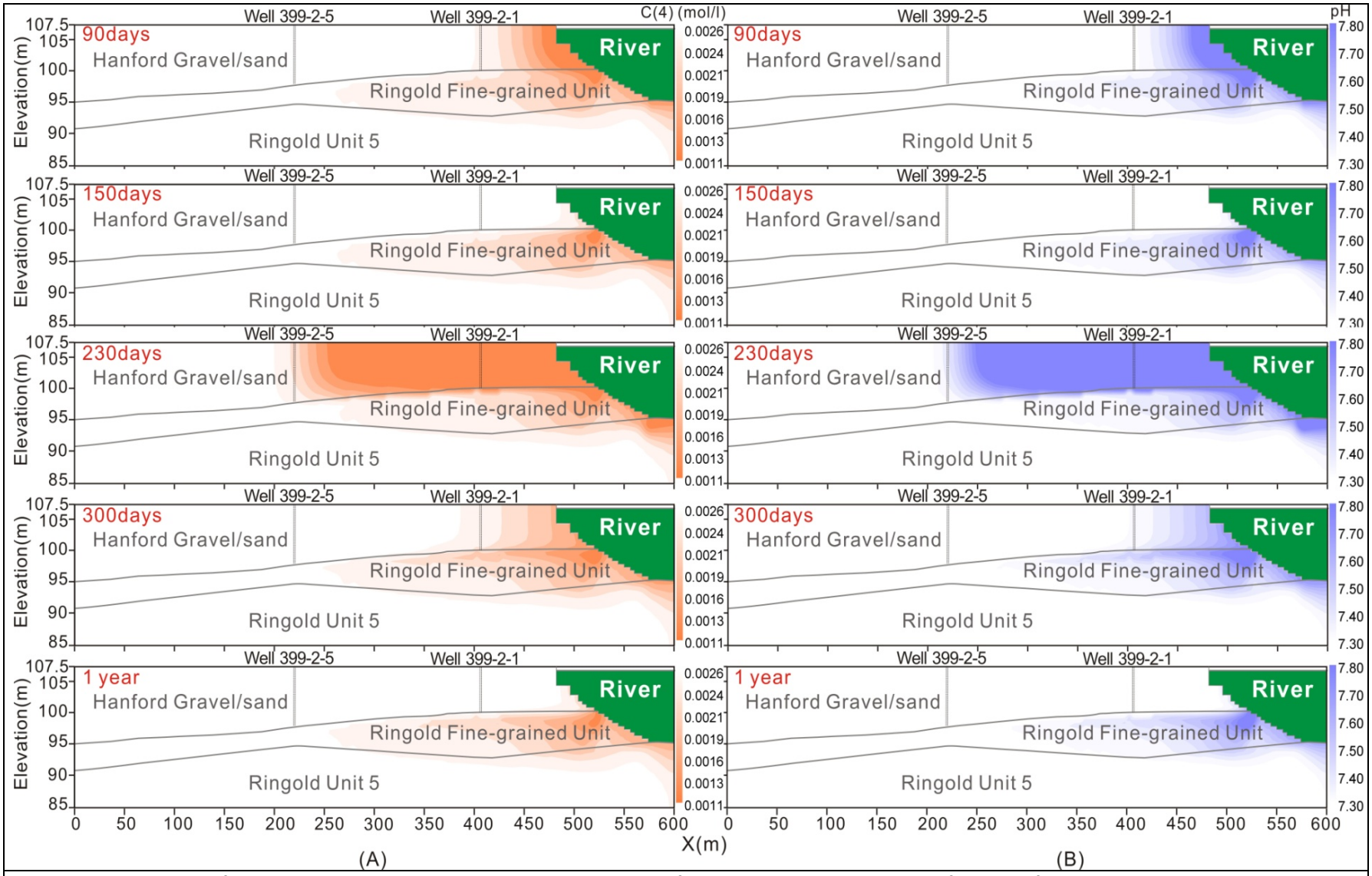

Figure 18. Illustration of the cross sectional model used to develop and test a field-scale multi-rate mass transfer model for U(VI) at the IFRC site. Shown are the simulated distributions of carbonate (A) and pH (B) during an annual cycle of river water intrusion and recession.

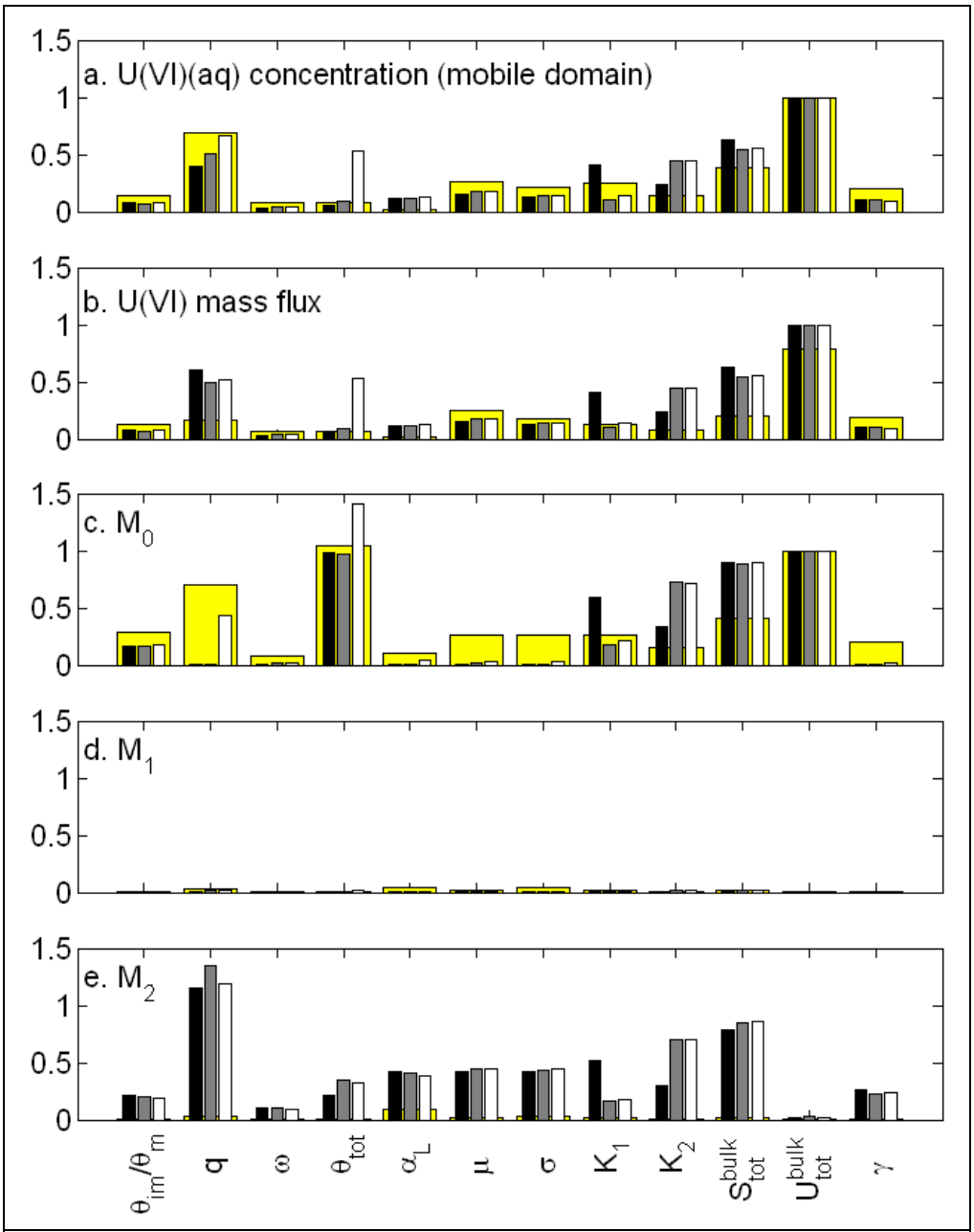

Figure 19. Laboratory scale composite sensitivities (yellow wide bars, background) and field scale composite sensitivities (thin bars, foreground), calculated from (a) concentrations, (b) mass flux, and (c) total mass M0, (d) center of mass M1 and (e) spreading of mass M2. The field scale sensitivities were calculated for synthetic groundwater composition (scenario 1 – black thin bars), average measured groundwater composition (scenario 2 – gray thin bars) and river water intrusion with average measured river water composition (scenario 3 – white thin bars).

Field-scale model for the natural attenuation of uranium at the Hanford 300 area using high performance computing

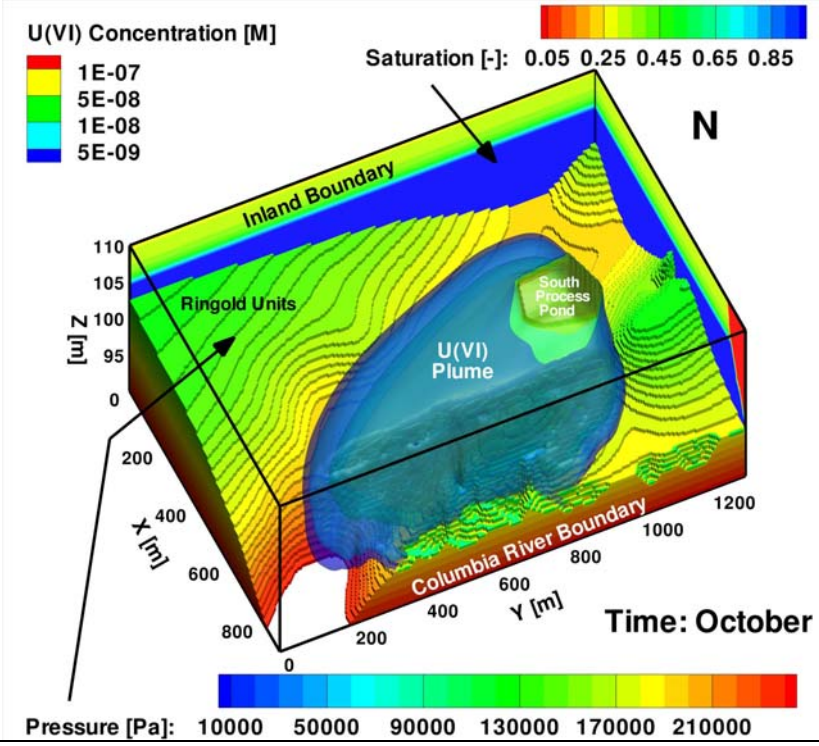

Figure 20. Three dimensional isosurfaces for the initial U(VI) concentration, saturation (side panels) and pressure painted on contact between the Hanford and Ringold formations. The domain size measures 900 m x 1300 m x 20 m.

The Hanford IFRC has been collaborating with a SciDAC project (P. Lichtner is principal investigator) to apply high performance computing to subsurface science issues associated with the 300 A U(VI) plume. Conceptual models, properties distributions, and process parameters and models are provided by the IFRC, while model set-up and calculations are performed by SciDAC. As part of this collaboration, three-dimensional simulations were carried out on a field-scale computational domain measuring 900 m x 1300 m x 20 m using grid spacing of 5 m in the x-and y-directions and 0.5 m in the z-direction (Figure 20). The computational domain is centered on the South Process Pond where the IFRC is located. Fifteen components or primary species were used to represent the chemical interactions in the system including aqueous speciation, adsorption and precipitation/dissolution reactions. A surface complexation model derived from Bond et al. (2008) was combined with the multi-rate model developed by Liu et al. (2008). Calculations involving over 28,000,000 degrees of freedom were performed on ORNL's Jaguar XT4 & 5 Cray supercomputers using 4096 processor cores. The runs were carried to one year simulation time requiring approximately 6 hours of cpu time. A detailed description of the model, calculations, and results has been submitted (Hammond and Lichtner, 2009).

This effort is an iterative one where evolving IFRC results are being integrated to yield a robust conceptual model for understanding present-day and future attenuation rates of U(VI) at the 300 Area site as needed by DOE/EM site stewards, remediation contractors, and others interested in the future disposition of the site. The conceptual model is based on the recognition of three distinct phases in the evolution of the site corresponding to: 1) initial emplacement of waste; 2) present-day conditions of slow leaching of labile U(VI)

from contaminated vadose and saturated zone sediments; and 3) the complete removal of non-labile U(VI) from the source region. The analysis reported here is focused on the second phase. Both labile and non-labile forms of U(VI) were included in the model as adsorbed and mineralized forms of U(VI), respectively. The non-labile form was important in providing a long-term source of U(VI). Rapid fluctuations in the Columbia River stage on hourly, weekly and seasonal time scales exerted strong control on the migration behavior of U(VI).

The calculations demonstrate that U(VI) is released into the Columbia River at a highly fluctuating rate in a ratchet-like behavior with nonzero U(VI) flux occurring only during flow from contaminated sediment into the river. The cumulative flux, however, is found to increase approximately linearly with time (Figure 21). The cumulative U(VI) flux to the river is compared for simulations using equilibrium surface complexation based on the Bond et al. (2008) model for different groundwater specific conductance values (dissolved bicarbonate), the Liu et al. (2008) multi-rate surface complexation model, and no adsorption. The resulting U(VI) flux of 25 kg/y for the best fit conductance coefficient is in reasonable agreement with measurements carried out at the site (Fritz and Arntzen, 2007; Robert Peterson, private comm.). The equilibrium and multi-rate sorption models gave similar results to the case with no sorption. These results are preliminary, and continued efforts will seek to embody the most robust and realistic site conceptual model into these calculations.

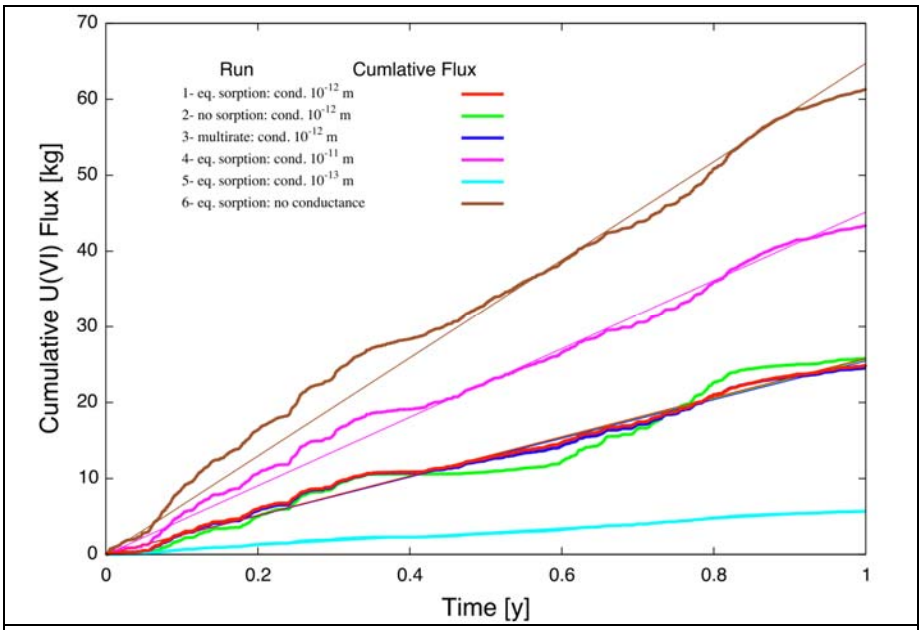

Figure 21. Plot of the U(VI) cumulative flux into the Columbia River with and without adsorption and different conductance coefficients at the river boundary. Mean rates in kg/y are: 64.72 (equilibrium adsorption, no cond.), 25.67 (no adsorption, cond. 10^{-12} m), 45.16 (equilibrium adsorption, cond. 10^{-11}), 25.47 (equilibrium adsorption, cond. 10^{-12} m), 5.81 (equilibrium adsorption, cond. 10^{-13} m), and 25.80 (multi-rate model, cond. 10^{-12} m).

Task 8. ERSD Outreach

ERSD Outreach (Site Interactions, Outreach, Etc.)

Several efforts were focused on outreach and communication to the outside community. In August, 2009, presentations on the Hanford IFRC and the PNNL Science Focus Area (SFA) were made to DOE Secretary Chu, Inez Triay (EM-1), and Washington State Senators Murray and Cantwell. Overall, the visit was highly positive and resulted in a white paper submitted to the DOE Richland Operations Site Manager, David Brockman, discussing the need for advances in deep vadose zone science in order to effectively manage and close the 200 A Central Plateau at Hanford.

Tours of the IFRC site were conducted for both DOE/EM management and project Principal Investigators of the new EM modeling initiative: "Advanced Subsurface Computing for Environmental Management (ASCEM)". The 300 Area IFRC is a potential demonstration site for the new modeling capabilities that will be developed by this project.

Jim McKinley and John Zachara presented a Hanford-wide seminar on the results of the spring 2009 deep vadose zone U(VI) mobilization experiment at the 300 Area IFRC to representatives of both DOE site offices (RL and ORP), regulators, and stakeholders on September 24, 2009. The presentation was well-received and considerable interaction and discussion occurred during and following the presentation on the implications of the results to future plume behavior and site remediation activities.

V. Non-IFRC Project Activities

Limited interactions have occurred with the staff conducting the CH2M Hill Plateau Remediation Contract (CPRC) polyphosphate infiltration project. To date, they have completed laboratory experiments and installed a field site north of the IFRC near the North Process Pond in the 300 Area. Interactions have been initiated with laboratory personnel performing feasibility experiments, and the field scientists that will be conducting and monitoring the experiment.

VI. Funding Issues

Project spending was on track with projection for the fourth quarter of FY 09 and there were no funding issues. The project carried over $374,217 K of FY 09 funding to FY 10 to facilitate continuing work in early FY 10, and pre-modeling and performance of the October 2009 U(VI) desorption injection experiment.

VII. Upcoming Plans/Issues

The following summarize plans for the first quarter of FY10 (October-December):

- Perform U reactive transport experiment by injecting water of lower U concentration during low Columbia River stage.

- Complete inversion of geophysics data for input to the hydrologic model
- Complete development of initial reactive transport model for U(VI) based on intact, saturated zone column experiments, and the passive and injection U field experiments.
- Integrate U(VI) reactive transport parameters derived from the intact column experiments into the updated IFRC field-scale transport model.
- Continue manuscript preparation, completion, and submission.

References

Bond, D. L., J. A. Davis, and J. M. Zachara. (2008) Uranium(VI) release from contaminated vadose zone sediments: estimation of potential contributions from dissolution and desorption. In *Adsorption of Metals by Geomedia II: Variables, mechanisms, and model applications*, Eds., M. O. Barnett and C. B. Kent, Elsevier: Amsterdam, 375-416.

Fritz, B. G. and E. V. Arntzen. (2007) Effect of rapidly changing river stage on uranium flux through the hyporheic zone. *Ground Water* 45(6), 753-760.

Hammond, G. E. and P. C. Lichtner. (2009) Field-scale model for the natural attenuation of uranium at the Hanford 300 area using high performance computing. *Water Resources Research* (Accepted).

Liu, C., J. M. Zachara, N. P. Qafoku, and Z. Wang. (2008) Scale-dependent desorption of uranium from contaminated subsurface sediments. Water Resour. Res., 44(W08413), doi:10.1029/2007WR006478.

VIII. Peer Reviewed Publications, Presentations, Posters, Abstracts, and Report

<u>Publications</u>

Hammond, G. E. and P. C. Lichtner. (2009) Field-scale model for the natural attenuation of uranium at the Hanford 300 area using high performance computing. *Water Resources Research* (Accepted).

Johnson, T., R. Versteeg, A. Ward, F. Day-Lewis, and A. Revil. (2009) Improved hydrogeophysical characterization and monitoring through parallel modeling and inversion of time-domain resistivity and induced polarization data. *Geophysics Journal* (Submitted).

Liu, C., Z. Shi, and J. M. Zachara. (2009) Kinetics of uranium(VI) Desorption from contaminated sediments: Effect of geochemical conditions and model evaluation. *Environ. Sci. Technol.,* 43, 6560-6566.

Rubin, Y., X. Chen, H. Murakami, and M. Hahn. (2009). A Bayesian approach for inverse modeling, data assimilation, and conditional simulation of spatial random fields. *Water Resources Research* (Submitted).

Presentations

Hammond, G. E., P. C. Lichtner and M. L. Rockhold. (2009) Stochastic Simulation of Uranium Migration at the Hanford 300 Area. Presented at the Migration '09 Conference, Kennewick, Washington, September 20-25, 2009.

Stoliker, D. L., D. B. Kent, J. A. Davis, and J. M. Zachara. (2009) Processes Controlling Rate and Transport of Uranium(VI) in Hanford's 300 Area. Presented at the 238th American Chemical Society National Meeting, Washington, DC, August 16-20, 2009.

Stoliker, D. L., D. B. Kent, J. A. Davis, and J. M. Zachara. (2009) Processes Controlling Rate and Transport of Uranium(VI) in Hanford's 300 Area. Presented at the Migration '09 Conference, Kennewick, Washington, September 20-25, 2009.

Zachara, J. M. (2009) Research to Understand Migration and Design Remediation: Focus on Tc, U, CCl_4, and Pu in 200A and River Corridor Settings. Presented by John Zachara (Invited Speaker) at Secretary Chu's Visit, Richland, Washington, August 12, 2009.

Zachara, J. M**.** (2009) Hanford 300 Area Integrated Field Research Challenge. Presented by John M. Zachara (Invited Speaker) at Secretary Chu's Visit, Richland, Washington, August 12, 2009.

Posters

Lee, J. H., J. K. Fredrickson, D. W. Kennedy, A. E. Plymale, A. Konopka, J. M. Zachara, X. Lin, and S. M. Heald. (2009) Biogeochemical Redox Transformations in Hanford 300 Area Subsurface Sediments. Presented at the Migration '09 Conference, Kennewick, Washington, September 20-25, 2009.

Liu, C., L. Zhong, and J. M. Zachara. (2009) Uranium(VI) Diffusion in Low Permeability Materials. Presented at the Migration '09 Conference, Kennewick, Washington, September 20-25, 2009.

.

McKinley, J. P., A. L. Ward, J. M. Zachara**,** V. R. Vermeul, C. T. Resch, and D. A. Moore. (2009) Geochemical Characterization as an Experimental Component in Determining Transport at the Hanford Site IFRC. Presented at the Migration '09 Conference, Kennewick, Washington, September 20-25, 2009.

McKinley, J. P., and J. M. Zachara. (2009) The Deep Vadose Zone as a Source Term for the 300 A U(VI) Plume. Presented at the Migration '09 Conference, Kennewick, Washington, September 20-25, 2009.

Abstracts

Draper, K. E., A. L. Ward, S. B. Yabusaki, C. J. Murray, and W. J. Greenwood**.** (2009) Abundances of Natural Radionuclides (40K, 238U, 232Th) in Hanford and Rifle Integrated Field Research Challenge Site Sediments and the Application to the Estimation of Grain Size Distributions. Abstract submitted to 2009 AGU Fall Meeting, San Francisco, California, December 15-19, 2009.

Freshley, M. D., J. S. Fruchter, E. M. Pierce, D. M. Wellman, and J. M. Zachara. (2009) Integration of Scientific Investigations and Remediation Decisions at the 300 Area, Hanford Site, Washington. Abstract Accepted at Waste Management Symposia 2010, Phoenix, Arizona, March 7-11, 2010.

Greenwood, W. J.**,** A. L. Ward, R. J. Versteeg, T. C. Johnson, and K. E. Draper. (2009) Azimuthal Resistivity Investigation of Anisotropic and Heterogeneity in an Unconfined Aquifer at the Hanford Integrated Field Research Challenge Site. Abstract submitted to 2009 AGU Fall Meeting, San Francisco, California, December 15-19, 2009.

Johnson T. C., R. J. Versteeg, A. L. Ward, C. E. Strickland, and W. J. Greenwood**.** (2009) Electrical Geophysical Characterization of the Hanford 300 Area Integrated Field Research Challenge using High Performance DC Resistivity Inversion Geostatistically Constrained by Borehole Conductivity Logs. Abstract submitted to 2009 AGU Fall Meeting, San Francisco, California, December 15-19, 2009.

Liu, C., J. M. Zachara, and J. P. McKinley. (2009) Scale-Dependent Contaminant Desorption Rates in Sediments. Abstract Accepted for Battelle Conference 2010, Remediation of Chlorinated and Recalcitrant Compounds, 7th International Conference, Monterey, California, May 24-27, 2010.

Ward A. L, R. J. Versteeg, C. E. Strickland, T. Fu, and V. R. Vermeul. (2009) Evaluation of Heat as a Tracer to Quantify Variations in Groundwater Velocities at Hanford's Integrated Field Research Challenge (IFRC) Site. Abstract submitted to 2009 AGU Fall Meeting, San Francisco, California, December 15-19, 2009.

Zachara, J. M., C. Zheng, D. B. Kent, J. K. Fredrickson, M. D. Freshley, G. E. Hammond, J. N. Christensen, A. Konopka, C. Liu, M. S. Conrad, J. P. McKinley, P. C. Lichtner, M. L. Rockhold, R. J. Versteeg, R. Haggerty, V. R. Vermeul, A. L. Ward, and Y. Rubin. (2009) Investigating In-Situ Mass Transfer Processes in a Groundwater U Plume Influenced by Groundwater-River Hydrologic and Geochemical Coupling. Abstract submitted to 2009 AGU Fall Meeting, San Francisco, California, December 15-19, 2009.

Zachara, J. M., B. N. Bjornstad, C. Zheng, D. B. Kent, J. K. Fredrickson, M. D. Freshley, G. E. Hammond, J. N. Christensen, A. Konopka, C. Liu, M. S. Conrad, J. P. McKinley, P. C. Lichtner, M. L. Rockhold, R. J. Versteeg, R. Haggerty, V. R. Vermeul, A. L. Ward, and Y. Rubin. (2009) Multiple Scale Studies to Understand Mass Transfer Controlled by.

(2009) Uranium Migration in a Dynamic Groundwater Plume Influenced by Water Table Fluctuations. Abstract submitted to 2009 AGU Fall Meeting, San Francisco, California, December 15-19, 2009.

Report

Pierce, E. M., M. D. Freshley, S. S. Hubbard, B. B. Looney, J. M. Zachara, L. Liang, D. Lesmes, G. M. Chamberlain, K. L. Skubal, V. Adams, M. E. Denham, and D. M. Wellman**.** (2009) *Scientific Opportunity to Reduce Risk in Groundwater and Soil Remediation.* PNNL-18516**,** Pacific Northwest National Laboratory, Richland, WA.